

Highly Conductive Poly(phenylene thienylene)s: *m*-Phenylene Linkages Are Not Always Bad

Changsik Song and Timothy M. Swager*

Department of Chemistry, Massachusetts Institute of Technology, Cambridge, Massachusetts 02139

Received January 26, 2005; Revised Manuscript Received March 28, 2005

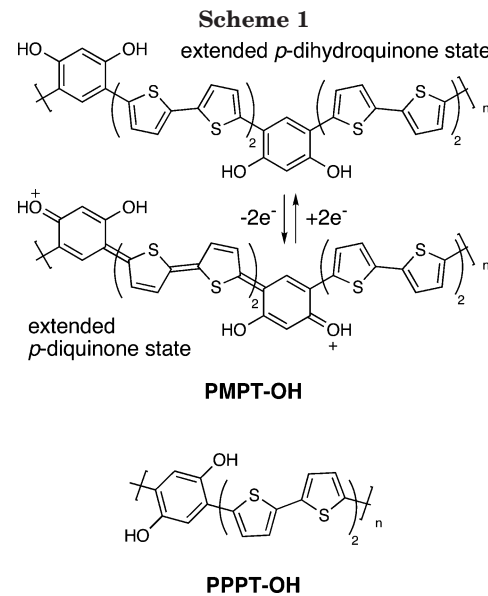
ABSTRACT: Two isomeric polymers, which contain *meta*- or *para*-phenylene linkages between conducting segments, have been synthesized and compared by electrochemical methods. The nonconjugated poly(1,5-diacetoxy-*m*-phenylene tetrathienylene) (PMPT-OAc) showed similar electroactivity to the *para*-isomer, poly(2,5-diacetoxy-*p*-phenylene tetrathienylene) (PPPT-OAc), in the cyclic voltammetry and in-situ conductivity measurements. Spectroelectrochemistry showed a similar buildup of sub-band-gap electronic transitions. Deacetylation of the polymers was performed successfully by reaction with hydrazine, producing PMPT-OH and PPPT-OH. Both phenol-substituted polymers exhibited greater electroactivity than the acetoxy-substituted polymers. In addition, the phenol substituents were found to lower the “turn-on” potential in the conductivity–potential profile for PMPT-OH, but not for PPPT-OH. An alkoxy-substituted PMPT-OMe shows electroactivity similar to that of PMPT-OAc in the cyclic voltammetry, in-situ conductivity, and spectroelectrochemistry.

Introduction

The demand for highly stable, highly conductive, and easily processable conjugated polymers in organic electronic and optoelectronic applications has led to extensive studies over the past two decades.¹ Major advances have been realized through novel design or synthetic modifications of conjugated polymers. For example, soluble and thus processable polythiophenes have been achieved by incorporating flexible substituents such as alkyl chains at the 3-position.^{2–4} Polythiophenes also have been electronically tuned by aid of electron-donating and/or electron-withdrawing substituents.^{4,5} Another approach is to modify the backbones by hybridizing thiénylenes with other conjugated molecules, such as various types of phenylenes.^{6,7} However, in the design of new highly electron/hole conductive polymers, *meta*-linkages between conducting segments are generally excluded because they interrupt conjugation. In fact, *meta*-linkages have usually been introduced in order to reduce conjugation in a tunable manner, for example, in synthesizing polymers with blue emission.⁸ It appears to be widely accepted that *meta*-linkages in polymers are something to be avoided if one wishes to produce systems with high conductivity that is generally associated with delocalized carriers.

Our group recently reported a calix[4]arene-based conducting polymer,⁹ which is not fully conjugated but instead contains electroactive segments between insulating bridges. In such a system, phenol groups were found to play a crucial role in the electropolymerization and the conduction pathway. The polymer also demonstrated an intriguing proton-dopable property, in which the segments were proposed to fluctuate between *p*-dihydroquinone-like and *p*-diquinone-like states (similar to what is shown for the materials of interest here in Scheme 1). Considering those features, phenol functionalities could be useful for designing conducting polymer sensors.

Our present study was motivated to investigate the potential of phenols as functional moieties in nonseg-



mented (i.e., those have a continuous interconnected π -system) conducting polymers. We proposed that, when strategically located, phenols would endow a nonconjugated *meta*-linked polymer with electroactive and conductive properties that are similar to, or even better than, those of a related *para*-isomer. In this study, two isomeric phenol containing polymers were prepared: poly(*m*-phenylene tetrathienylene)s (PMPTs) and poly(*p*-phenylene tetrathienylene)s (PPPTs) (Scheme 1). In PMPTs, when they are oxidized, it is plausible that the charges are localized on the phenolic oxygens. Upon oxidation, the initially nonconjugated backbone becomes highly delocalized with both aromatic and quinoid structures in the same chain, a scheme that has been utilized in the design of small-band-gap polymers.¹⁰ In this work, a series of PMPTs and PPPTs were synthesized and characterized by several electrochemical methods. The in-situ conductivities of two isomeric polymers were compared by using interdigitated microelectrodes,¹¹ and their electronic transitions were also compared by UV-vis spectroelectrochemistry.

* Corresponding author. E-mail: tswager@mit.edu.

Experimental Section

Instrumentation. NMR spectra were recorded on a Varian Mercury-300, Bruker Advance-400, or Varian Inova-500 spectrometer. Chemical shifts are referenced to residual solvent peaks. High-resolution mass spectra (HR-MS) were obtained on a Bruker Daltonics APEX II 3T FT-ICR-MS. Electrochemical studies were carried out using an Autolab PGSTAT 10 or PGSTAT 20 potentiostat (Eco Chemie) in a three-electrode cell configuration consisting of a quasi-internal Ag wire reference electrode (BioAnalytical Systems) submerged in 0.01 AgNO₃/0.1 M tetrabutylammonium hexafluorophosphate (TBAPF₆) in anhydrous CH₃CN, a Pt button (1.6 mm in diameter), 5 μm interdigitated Pt micro, ITO-coated glass (100 Ω sheet resistance), or Au-coated poly(ethylene terephthalate) (PETE) electrode as the working electrode, and a Pt coil or Pt gauze as the counter electrode. The ferrocene/ferrocenium (Fc/Fc⁺) redox couple was used as a reference. Half-wave potentials of Fc/Fc⁺ were observed between 210 and 245 mV vs Ag/Ag⁺ in CH₂Cl₂ and 80 mV in CH₃CN. For the in-situ conductivity measurements, polymer films were electrochemically deposited on 5 μm interdigitated Pt microelectrodes and placed in a monomer-free solution. Drain current measurements were typically carried out at a 5 mV/s scan rate with a 40 mV offset potential between the two working electrodes. The conductivity was then calculated from the value of the drain current by applying geometrical factors¹¹ and also corrected with a known material, poly(3-methylthiophene), at 60 S/cm. The polymer film thickness for the conductivity calculation was measured with a surface profilometer (Veeco Dektak 6M Stylus Profiler). The baseline (A) of a bare interdigitated microelectrode was first obtained. Next, the surface profile (B) of a given polymer film on the electrode was measured. Several values of A and B were taken to get averages of each. The thickness was determined by subtracting the averaged value of A from the averaged value of B. Absorption spectra for spectroelectrochemistry were obtained using a HP 8453 diode array spectrometer. FT-IR spectra of polymer films were taken using Nicolet 8700 FT-IR spectrometer with a fixed 30° specular reflectance accessory.

Materials. Spectroscopic grade CH₂Cl₂ and CH₃CN were purchased from Aldrich for electrochemistry. TBAPF₆ was recrystallized in ethanol prior to use. 4,6-Diiodobenzene-1,3-diol,¹² 2,5-diiodobenzene-1,4-diol,¹³ and 5-tributylstannyl-2,2'-bithiophene¹⁴ were prepared by literature methods. Anhydrous DMF was purchased from Aldrich as Sure-Seal Bottles and used as received. All other chemicals were of reagent grade and used as received.

1,5-Diacetoxy-2,4-diiodobenzene (1b). In a 100 mL round-bottom flask equipped with a stir bar were combined 4,6-diiodobenzene-1,3-diol (1.08 g, 3 mmol), acetic anhydride (1.42 mL, 15 mmol), and 5 mL of pyridine. After being stirred overnight at room temperature, the mixture was poured into water and extracted with diethyl ether. The organic layer was washed with brine, dried over MgSO₄, and evaporated under reduced pressure. The resulting crude product was purified by column chromatography (ethyl acetate:hexane 1:1). Yield: 1.30 g of white solid (97%). ¹H NMR (300 MHz, CDCl₃) δ: 8.26 (s, 1H), 6.97 (s, 1H), 2.36 (s, 6H). ¹³C NMR (100 MHz, CDCl₃) δ: 168.1, 152.2, 147.7, 118.1, 88.1, 21.4. HR-MS (ESI): calcd for C₁₀H₈I₂O₄ [M + Na]⁺, 468.8404; found, 468.8383.

1,4-Diacetoxy-2,5-diiodobenzene. Similar to the synthesis of **1b** except using 2,5-diiodobenzene-1,4-diol. Yield: 1.09 g of white solid (82%). ¹H NMR (400 MHz, CDCl₃) δ: 7.53 (s, 2H), 2.36 (s, 6H). ¹³C NMR (100 MHz, CDCl₃) δ: 168.4, 149.6, 132.7, 90.2, 21.3. HR-MS (ESI): calcd for C₁₀H₈I₂O₄ [M + Na]⁺, 468.8404; found, 468.8416.

1,5-Bis(tert-butyldimethylsilyloxy)-2,4-diiodobenzene (1c). In a 100 mL round-bottom flask equipped with a stir bar were combined 4,6-diiodobenzene-1,3-diol (1.45 g, 4 mmol), TBDMSCl (1.8 g, 12 mmol), and 20 mL of anhydrous DMF under Ar. After being stirred for 10 min, imidazole (1.38 g, 20 mmol) was added to the mixture, and it was stirred overnight at room temperature. The mixture was poured into water and extracted with diethyl ether. The organic layer was

then washed with brine, dried over MgSO₄, and evaporated under reduced pressure. The resulting crude product was purified by column chromatography (dichloromethane:hexane 1:15). Yield: 2.30 g of white solid (97%). ¹H NMR (400 MHz, CDCl₃) δ: 8.04 (s, 1H), 6.40 (s, 1H), 1.07 (s, 18H), 0.28 (s, 12H). ¹³C NMR (100 MHz, CDCl₃) δ: 156.4, 147.1, 109.5, 81.3, 26.0, 18.6, -3.8. HR-MS (ESI): calcd for C₁₈H₃₂I₂O₂Si₂ [M + Na]⁺, 612.9922; found, 612.9895.

1,4-Bis(tert-butyldimethylsilyloxy)-2,5-diiodobenzene. Similar to the synthesis of **1c** except using 2,5-diiodobenzene-1,4-diol. Yield: 2.34 g of white solid (99%). ¹H NMR (400 MHz, CDCl₃) δ: 7.18 (s, 2H), 1.05 (s, 18H), 0.26 (s, 12H). ¹³C NMR (100 MHz, CDCl₃) δ: 150.4, 128.0, 89.7, 26.1, 18.5, -3.9. HR-MS (ESI): calcd for C₁₈H₃₂I₂O₂Si₂ [M + Na]⁺, 612.9922; found, 612.9904.

1,5-Dimethoxy-2,4-diiodobenzene (1d). In a 100 mL round-bottom flask equipped with a stir bar were combined 4,6-diiodobenzene-1,3-diol (1.09 g, 3 mmol), K₂CO₃ (4.15 g, 30 mmol), and 30 mL of DMF under Ar. Iodomethane (0.936 mL, 15 mmol) was slowly added to the mixture, and it was stirred for 6 h at room temperature. The mixture was diluted with ethyl acetate, and the organic layer was washed with water and brine, dried over MgSO₄, and evaporated under reduced pressure. The resulting crude product was filtered through a pad of silica gel, eluting with dichloromethane. The solvent was evaporated under reduced pressure, and the resulting solid was further purified by recrystallization (dichloromethane, hexane). Yield: 1.07 g of white solid (91%). ¹H NMR (400 MHz, CD₂Cl₂) δ: 8.03 (s, 1H), 6.40 (s, 1H), 3.88 (s, 6H). ¹³C NMR (100 MHz, CD₂Cl₂) δ: 160.3, 147.3, 96.4, 75.5, 57.0. HR-MS (ESI): calcd for C₈H₈I₂O₂ [M + Na]⁺, 412.8506; found, 412.8522.

1,5-Diacetoxy-2,4-bis(2,2'-bithiophen-5-yl)benzene (2b). In a Schlenk tube equipped with a stir bar were combined **1b** (0.446 g, 1 mmol), Pd₂(dba)₃ (31 mg, 3 mol %), P(t-Bu)₃ (24 mg, 6.6 mol %), and 10 mL of toluene under Ar. To the mixture was added 5-tributylstannyl-2,2'-bithiophene (1.37 g, 3 mmol) and stirred for 48 h at 80 °C. The reaction mixture was then cooled to room temperature, diluted with ethyl acetate, and filtered through a pad of silica gel. The silica gel was thoroughly washed with ethyl acetate, and the solvent was evaporated under reduced pressure. The crude solid was washed with diethyl ether and then further purified by recrystallization (dichloromethane, hexane). Yield: 0.262 g of pale yellow solid (50%). ¹H NMR (300 MHz, CD₂Cl₂) δ: 7.91 (s, 1H), 7.32 (d, 2H, J = 3.8 Hz), 7.29 (dd, 2H, J = 5.3, 1.1 Hz), 7.25 (dd, 2H, J = 3.6, 1.1 Hz), 7.21 (d, 2H, J = 3.8 Hz), 7.07 (s, 1H), 7.06 (dd, 2H, J = 5.3, 3.6 Hz), 2.36 (s, 6H). ¹³C NMR (100 MHz, CD₂Cl₂) δ: 169.3, 146.6, 139.0, 137.4, 136.4, 129.5, 128.5, 127.7, 126.0, 125.4, 124.55, 124.52, 119.4, 21.8. HR-MS (ESI): calcd for C₂₆H₁₈O₄S₄ [M + Na]⁺, 544.9980; found, 544.9999.

1,5-Bis(tert-butyldimethylsilyloxy)-2,4-bis(2,2'-bithiophen-5-yl)benzene (2c). In a Schlenk tube equipped with a stir bar were combined **1c** (1.18 g, 2 mmol), Pd₂(dba)₃ (104 mg, 5 mol %), P(t-Bu)₃ (81 mg, 0.4 mmol), and 15 mL of toluene under Ar. To the mixture was added 5-tributylstannyl-2,2'-bithiophene (2.73 g, 6 mmol) and stirred for 48 h at 80 °C. The reaction mixture was then cooled to room temperature, diluted with ethyl acetate, and filtered through a pad of silica gel. The silica gel was thoroughly washed with ethyl acetate, and the solvent was evaporated under reduced pressure. The crude solid was washed with cold hexane and then further purified by recrystallization (dichloromethane, hexane). Yield: 0.872 g of yellow solid (65%). ¹H NMR (400 MHz, CDCl₃) δ: 7.72 (s, 1H), 7.25 (d, 2H, J = 3.6 Hz), 7.21 (dd, 2H, J = 5.2, 1.2 Hz), 7.18 (dd, 2H, J = 3.6, 1.2 Hz), 7.15 (d, 2H, J = 3.6 Hz), 7.04 (dd, 2H, J = 5.2, 3.6 Hz), 6.53 (s, 1H), 1.00 (s, 18H), 0.27 (s, 12H). ¹³C NMR (100 MHz, CDCl₃) δ: 152.4, 138.7, 138.2, 136.4, 129.4, 128.0, 125.8, 124.1, 123.6, 123.2, 119.6, 111.5, 26.2, 18.8, -3.6. HR-MS (ESI): calcd for C₃₄H₄₂O₂S₄Si₂ [M + H]⁺, 667.1679; found, 667.1683.

1,5-Dimethoxy-2,4-bis(2,2'-bithiophen-5-yl)benzene (2d). In a Schlenk tube equipped with a stir bar were combined **1d** (0.390 g, 1 mmol), Pd₂(dba)₃ (31 mg, 3 mol %), P(t-Bu)₃ (13 mg, 6.6 mol %), LiCl (170 mg, 4 mmol), and 10 mL of DMF

under Ar. To the mixture was added 5-triptylstannyl-2,2'-bithiophene (1.37 g, 3 mmol) and stirred overnight at room temperature. The reaction mixture was diluted with dichloromethane and filtered through a pad of silica gel. Most of the solvent was evaporated under reduced pressure. The residue was diluted with ethyl acetate, washed with brine ($\times 2$), dried over $MgSO_4$, and evaporated under reduced pressure. The resulting residue was precipitated with hexane, and the crude solid was washed with copious amounts of hexane. The product was further purified by recrystallization (dichloromethane, hexane). Yield: 0.347 g of yellow solid (74%). 1H NMR (400 MHz, CD_2Cl_2) δ : 7.89 (s, 1H), 7.38 (d, 2H, J = 3.8 Hz), 7.23–7.25 (m, 4H), 7.18 (d, 2H, J = 3.8 Hz), 7.05 (dd, 2H, J = 5.1, 3.7 Hz), 6.64 (s, 1H), 4.00 (s, 6H). ^{13}C NMR (100 MHz, CD_2Cl_2) δ : 156.7, 138.6, 138.2, 136.7, 128.4, 127.7, 125.6, 124.6, 124.0, 123.7, 116.4, 96.7, 56.4. HR-MS (ESI): calcd for $C_{24}H_{18}O_2S_4$ [M] $^+$, 466.0184; found, 466.0176.

1,3-Bis(2,2'-bithiophen-5-yl)benzene (3). In a Schlenk tube equipped with a stir bar were combined 1,3-diiodobenzene (0.337 g, 1 mmol), $PdCl_2(PPh_3)_2$ (37 mg, 5 mol %), and 10 mL of toluene under Ar. To the mixture was added 5-triptylstannyl-2,2'-bithiophene (1.37 g, 3 mmol) and stirred overnight at 80 °C. The reaction mixture was then cooled to room temperature, diluted with dichloromethane, and filtered through a pad of silica gel. The solvent was evaporated under reduced pressure, and the resulting residue was precipitated with hexane. The crude solid was washed with hexane and further purified by recrystallization (dichloromethane, hexane). Yield: 0.350 g of bright yellow solid (86%). 1H NMR (400 MHz, CD_2Cl_2) δ : 7.83 (pseudo-t, 1H, J = 1.7 Hz), 7.54 (dd, 2H, J = 7.7, 1.7 Hz), 7.41 (t, 1H, J = 7.7 Hz), 7.33 (d, 2H, J = 3.8 Hz), 7.27 (dd, 2H, J = 5.1, 1.1 Hz), 7.25 (dd, 2H, J = 3.7, 1.1 Hz), 7.20 (d, 2H, J = 3.8 Hz), 7.06 (dd, 2H, J = 5.1, 3.7 Hz). ^{13}C NMR (100 MHz, CD_2Cl_2) δ : 142.9, 137.7, 137.6, 135.2, 130.1, 128.5, 125.2, 125.1, 124.8, 124.3, 123.0. HR-MS (ESI): calcd for $C_{22}H_{14}S_4$ [M] $^+$, 407.0051; found, 407.0042.

1,4-Diacetoxy-2,5-bis(2,2'-bithiophen-5-yl)benzene (4b). In a Schlenk tube equipped with a stir bar were combined 1,4-diacetoxy-2,5-diiodobenzene (0.446 g, 1 mmol), $PdCl_2(PPh_3)_2$ (37 mg, 5 mol %), and 10 mL of toluene under Ar. To the mixture was added 5-triptylstannyl-2,2'-bithiophene (1.37 g, 3 mmol) and stirred overnight at 80 °C. The product precipitated as the reaction progressed. The reaction mixture was then cooled to room temperature. The product was filtered out and washed thoroughly with diethyl ether. The crude product was then redissolved with dichloromethane and passed through a pad of silica gel. The silica gel was thoroughly washed with dichloromethane, and the solvent was evaporated under reduced pressure. The resulting solid was then further purified by recrystallization (dichloromethane, hexane). Yield: 0.429 g of pale yellow solid (82%). 1H NMR (500 MHz, THF- d_8) δ : 7.60 (s, 2H), 7.43 (d, 2H, J = 3.8 Hz), 7.37 (m, 2H), 7.29 (m, 2H), 7.23 (d, 2H, J = 3.8 Hz), 7.04 (dd, 2H, J = 5.0, 3.5 Hz), 2.38 (s, 6H). ^{13}C NMR (125 MHz, THF- d_8) δ : 169.0, 145.5, 139.7, 138.0, 136.9, 128.9, 128.2, 127.6, 126.0, 124.92, 124.86, 124.1, 21.5. HR-MS (ESI): calcd for $C_{26}H_{18}O_4S_4$ [M] $^+$, 544.9980; found, 544.9992.

1,4-Bis(tert-butylidimethylsilyloxy)-2,5-bis(2,2'-bithiophen-5-yl)benzene (4c). In a Schlenk tube equipped with a stir bar were combined 1,4-bis(tert-butylidimethylsilyloxy)-2,5-diiodobenzene (0.177 g, 0.3 mmol), $PdCl_2(PPh_3)_2$ (11 mg, 5 mol %), and 3 mL of toluene under Ar. To the mixture was added 5-triptylstannyl-2,2'-bithiophene (0.341 g, 0.75 mmol) and stirred for 20 h at 80 °C. The product precipitated as the reaction progressed. The reaction mixture was then cooled to room temperature. The product was filtered out and washed thoroughly with ethyl acetate. The crude product was then redissolved with dichloromethane and passed through a pad of silica gel. The silica gel was thoroughly washed with dichloromethane, and the solvent was evaporated under reduced pressure. The resulting solid was then further purified by recrystallization (dichloromethane, hexane). Yield: 0.194 g of pale yellow solid (97%). 1H NMR (400 MHz, $CDCl_3$) δ : 7.32 (d, 2H, J = 3.8 Hz), 7.23 (dd, 2H, J = 5.2, 1.0 Hz), 7.21 (dd, 2H, J = 3.6, 1.0 Hz), 7.16 (d, 2H, J = 3.8 Hz), 7.15 (s, 2H),

7.05 (dd, 2H, J = 5.2, 3.6 Hz), 1.03 (s, 18H), 0.27 (s, 12H). ^{13}C NMR (100 MHz, $CDCl_3$) δ : 146.4, 138.6, 138.0, 137.2, 128.1, 126.4, 124.8, 124.4, 123.8, 123.5, 119.6, 26.3, 18.8, -3.5. HR-MS (ESI): calcd for $C_{34}H_{42}O_2S_4Si_2$ [M] $^+$, 667.1679; found, 667.1706.

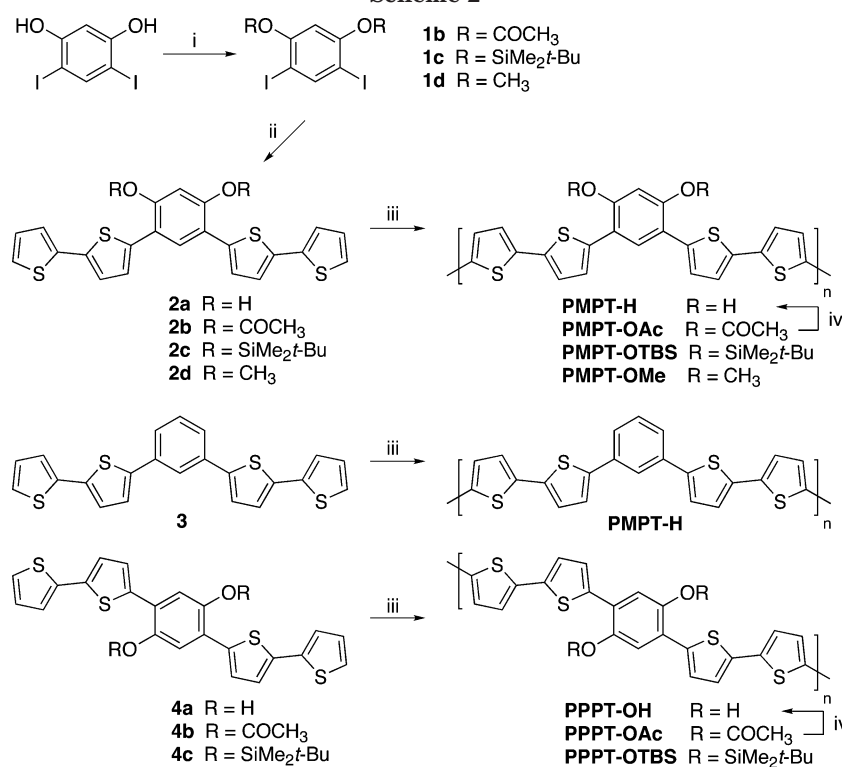
Results and Discussion

Monomer Synthesis. The syntheses of the monomers are outlined in Scheme 2. Attempts to synthesize the *meta*-linked monomer **2a** by Stille coupling between 4,6-diiodoresorcinol and 5-tri-*n*-butylstannyl-2,2'-bithiophene failed. Subsequently, the phenol groups were protected with acetyl or TBDSM groups. Although protected monomers **2b,c** could be obtained by Stille coupling in good to high yields, deprotection to **2a** was complicated by its instability to air, giving black intractable products. Therefore, removal of the protecting group was carried out in postpolymerization modification. For comparison, an *O*-alkyl version **2d**, a nonsubstituted version **3**, and *para*-linked isomers **4b,c** were synthesized under similar conditions.

Electropolymerization.¹⁵ All monomers were polymerized via oxidative coupling under swept potential conditions. Electropolymerizations were performed in CH_2Cl_2 solutions containing ca. 2 mM of monomers and 0.1 M of $TBAPF_6$ as a supporting electrolyte. In most cases, CH_2Cl_2 proved to be a good solvent for electropolymerization. However, when monomers were too soluble in CH_2Cl_2 (**2c** or **4c**) or when the working electrode had a large surface area (ITO-coated glass electrode or gold-coated PETE), a significant amount of the resulting polymer failed to be deposited onto the electrode. This could be attributed to the solubility of initially coupled oligomers. This effect was especially evident when *O*-TBDMS versions (**2c** or **4c**) were polymerized in CH_2Cl_2 . It was observed that oxidized oligomers diffused away from the electrode surface. This problem was overcome by adding CH_3CN , a poor solvent. Depending on the solubility of each monomer, a 1:1 to 1:3 mixture of CH_2Cl_2 : CH_3CN was used for electropolymerizations.

Figure 1 shows the cyclic voltammograms (CVs) during the polymerization of **2b** and **4b**. The initial oxidation of monomer **2b** occurred at a potential slightly higher than **4b**, reflecting the nonconjugated nature of the *meta*-linkage. For both materials, all subsequent scans displayed much lower potential oxidation onsets, thereby indicating that electroactive polymer had deposited onto the electrode. The oxidation peak potential of poly(**2b**) (PMPT-OAc) and poly(**4b**) (PPPT-OAc) were minimally different. Table 1 summarizes the electrochemical results for monomers (**2b–d, 3, 4b,c**) and their polymers. As expected, the electron-donating effect of methoxy groups results in a lower oxidation potential for monomer **2d**. The *O*-TBDMS versions **2c** and **4c** also oxidized at low potentials for the same reason.

Deprotection To Give Free –OH Groups. PMPT-OAc and PPPT-OAc were chosen to generate free –OH versions, PMPT-OH and PPPT-OH, respectively, because the acetyl groups can be easily removed by addition of hydrazine. As-grown polymer films on several types of electrodes were exposed to hydrazine vapor, under which the films immediately became crimson in color. After ca. 15 min, the films were washed with copious amounts of MeOH and then with CH_2Cl_2 . Figures 2 and 3 show the FT-IR and UV-vis spectra, respectively, of films before and after exposure to hydrazine. It is clearly observed that the strong C=O

Scheme 2^a

^a (i) Acetic anhydride, pyridine, RT. (1b); TBDMSCl, imidazole, DMF, RT. (1c); MeI, K₂CO₃, DMF, RT. (1d) (ii) 5-Tri-n-butylstannyln-2,2'-bithiophene, Pd cat., toluene or DMF, 80 °C or RT. (iii) Electropolymerization under swept potential conditions in CH₂Cl₂ containing ca. 2 mM of monomers and 0.1 M TBAPF₆ as a supporting electrolyte. (iv) Hydrazine, RT.

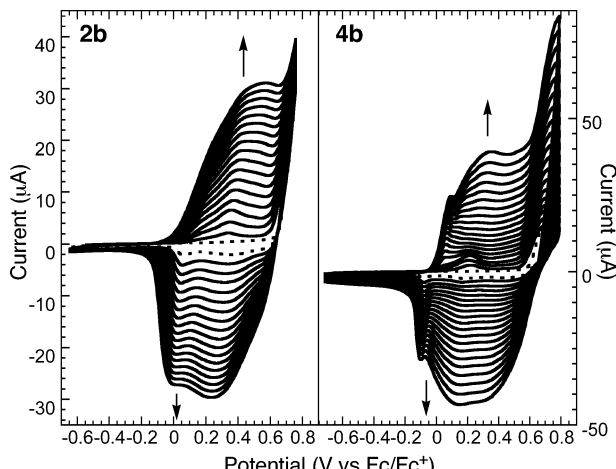


Figure 1. Electropolymerization (100 mV/s) of **2b** (left) and **4b** (right) on Pt button electrodes in CH₂Cl₂ with 0.1 M TBAPF₆ as a supporting electrolyte. Dotted lines represent the first scan.

vibration disappeared after exposure to hydrazine. The weaker than expected C–H and O–H stretching vibrations in spectra C and D in Figure 2 are a result of the thin nature of the films grown from PPPT-OAc and PPPT-OH, which results in broad and weak signals. The hydrazine reaction did not significantly affect the UV-vis absorption (Figure 3); hence, we conclude the acetyl groups were successfully removed to leave free –OH without degradation of the polymer structure.

Polymer Electrochemistry Comparisons of Meta vs Para. Figure 4 compares the CVs of the PMPTs and the PPPTs. We observed two broad, poorly resolved oxidation and reduction peaks in both PMPT-OAc and PPPT-OAc, and their CVs were quite similar, with the

Table 1. Electrochemical Results: Monomer Oxidation Potentials ($E_{a,m}$) and Polymer Oxidation/Reduction Potentials ($E_{a,p}/E_{c,p}$)

| monomer | $E_{a,m}$ (V) ^a | $E_{a,p}$ (V) | $E_{c,p}$ (V) |
|-----------------------|----------------------------|------------------|---------------|
| 2b^b | >0.8 | 0.41, 0.68 | 0.05, 0.33 |
| 2c^c | 0.57 | 0.12, >1.0 | 0.14 |
| 2d^d | 0.47 | 0.37, 0.61 | 0.01, 0.41 |
| 3^b | 0.81 | >1.0 | -0.10 |
| 4b^b | 0.69 | 0.20, 0.36, 0.72 | -0.18, 0.18 |
| 4c^c | 0.48 | 0.74 | 0.41 |

^a All potentials measured vs Fc/Fc⁺ at scan rate 100 mV/s.
^b Performed in CH₂Cl₂. ^c Performed in a mixed solvent of CH₂Cl₂ and CH₃CN. ^d Performed in CH₃CN.

exception of the first oxidation peak. Interestingly for PPPT-OAc, we observed a well-resolved low-potential redox couple, similar to those reported for polythiophenes with long alkoxy substituents.^{5,6} We also observed that this redox couple was more pronounced at low scan rates and thin films. This is most evident for the reduction cycle of PPPT-OAc, which suggests that it is more sensitive to ion diffusion or that a structural relaxation has occurred in the oxidized state. However, after the first oxidation, the electrochemistry of both O-Ac polymers became similar, which suggests that the lone pairs of the acetoxy groups in PMPT-OAc are capable of contributing to the delocalization suggested in Scheme 1.

Deprotection of the acetyl groups changed the electrochemistry of the polymers dramatically, especially for PMPT-OAc. For PPPT-OAc we observed a broader electroactivity and a loss of the low-potential redox activity shown for PPPT-OAc. The oxidation onset potential of PPPT-OH remained approximately the same as that of PPPT-OAc. In contrast, the oxidation onset potential of PMPT-OH shifted to lower potential, and the polymer's

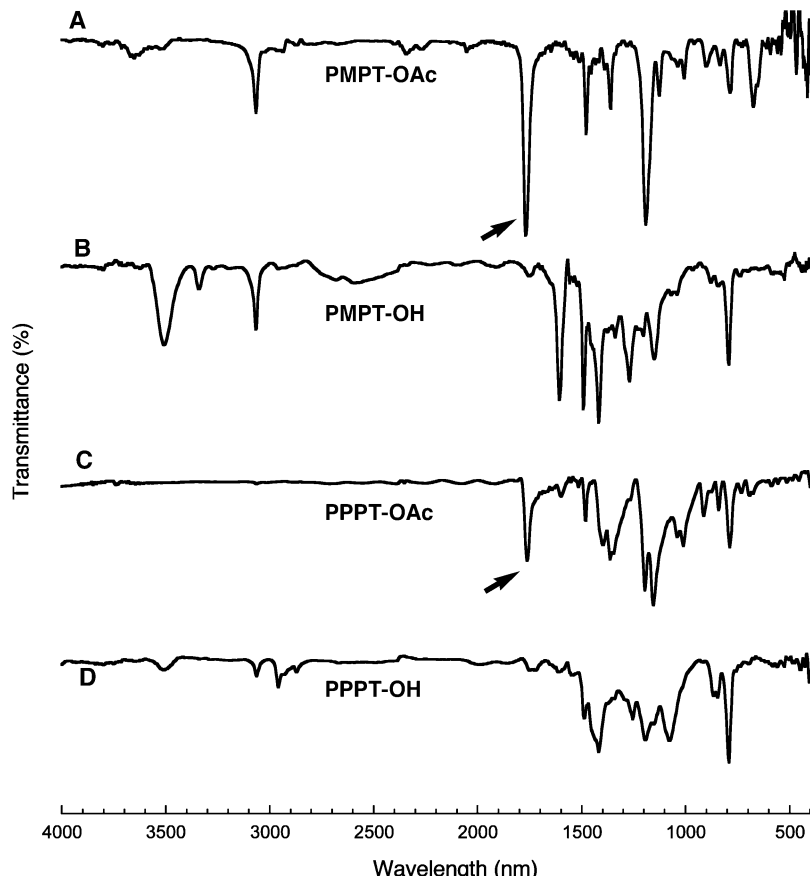


Figure 2. Specular reflectance FT-IR spectra of PMPT-OH (B) and PPPT-OH (D). The strong C=O stretchings (arrows) of PMPT-OAc (A) and PPPT-OAc (C) disappeared when exposed to hydrazine. The spectra were measured from films deposited onto gold-coated PETE.

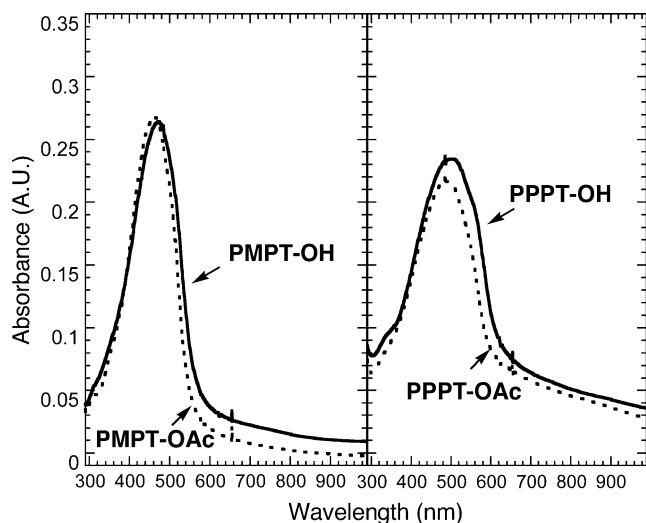


Figure 3. UV-vis spectra of PMPT-OH (left; solid line) and PPPT-OH (right; solid line). Dotted lines represent UV-vis absorption of PMPT-OAc (left) and PPPT-OAc (right). The spectra were measured from films deposited onto ITO-coated glass.

CV was much broader than the acetate derivative. This latter feature is attributed to the formation of extended *p*-diquinone states that are more favored in the deprotected form because of the superior ability of the -OH group to stabilize positive charges. Although the free -OH substituents seemed to improve the polymers' electroactivity, oxidized PMPT-OH and PPPT-OH were not stable under ambient conditions. All electrochemical

measurements of those polymers were performed in a glovebox under a nitrogen atmosphere.

Meta vs Para in-Situ Conductivity Measurement. It is not surprising, considering the similarity of the CVs, that we find the conductivity of the *meta*-linked PMPT-OAc is of the same order of magnitude as the *para*-linked PPPT-OAc (Figure 5). In the potential-conductivity profile of PMPT-OAc, the conductivity increased rapidly from ca. 0 V and reached a plateau above ca. 0.3 V (vs Fc/Fc⁺). The conductivity profile of PPPT-OAc behaved in a similar manner. This conductivity plateau results from the limit of an interchain charge hopping process.^{16,17} As in the case of polythiophenes, the interchain charge transport in PMPTs and PPPTs operates due to the proximity of the polymer backbones, providing multichannel electronic connectivity. It would appear that the *meta*-linkages do not hamper the conduction pathway in this system.

The shapes of potential-conductivity profile of the -OH versions, PMPT-OH and PPPT-OH, resembled their acetate versions (Figure 6). In PPPT-OH, the drain current, which is proportional to conductivity, "turns on" at almost the same potential as PPPT-OAc. In contrast, the drain current onset is at a much lower potential for PMPT-OH. As mentioned above, the free -OH appears to facilitate the formation of extended *p*-diquinone states.

Meta vs Para Spectroelectrochemistry. UV-vis spectroelectrochemical studies further reveal that *meta*-linkages produce delocalized electronic structures when the polymers are oxidized. Figure 7 shows in-situ measurements of the UV-vis absorption of polymers

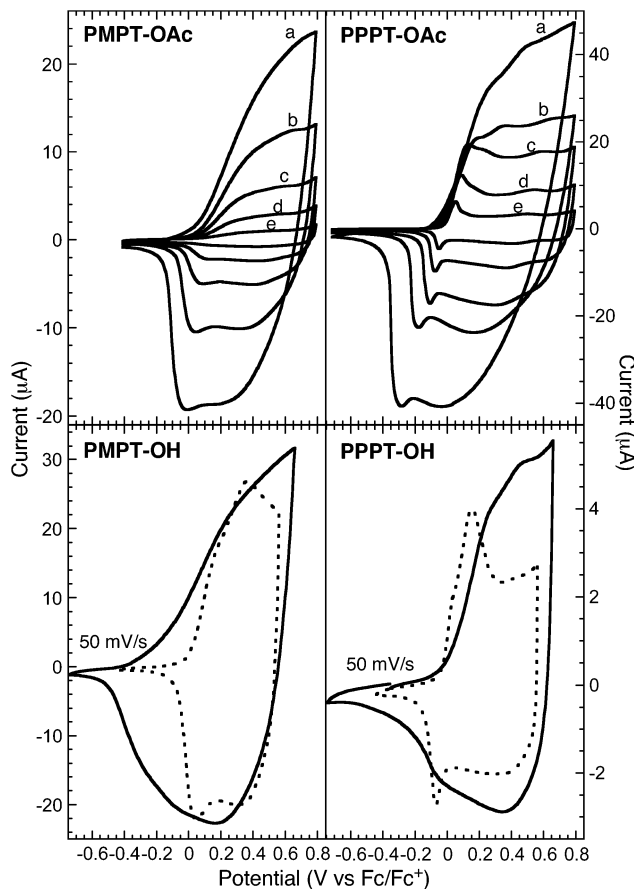


Figure 4. (top) CVs of PMPT-OAc (left) and PPPT-OAc (right) at different scan rates: (a) 200, (b) 100, (c) 50, (d) 25, and (e) 10 mV/s. (bottom) CVs of PMPT-OH (left) and PPPT-OH (right). Dotted line represents the CV before exposure to hydrazine. All measurements were carried out in CH₂Cl₂ with 0.1 M TBAPF₆ onto Pt button electrodes.

deposited onto ITO-coated glass electrodes. Because of the instability of the oxidized PMPT-OH and PPPT-OH, only the acetate versions were measured. The UV-vis spectra of PPPT-OAc show a decrease of the original band-gap transition and the buildup of intragap energy states, which appear very similar to those observed for alkoxy-substituted poly(phenylene bisthiophene)s.⁶ This matches well to polaron–bipolaron model¹⁸ of charge-delocalized π -platforms. It should be noted that even in the nonconjugated PMPT-OAc similar electronic states develop and more delocalized energy states build up at lower applied potentials.

Substituent Effects in PMPTs. To further investigate the electronic properties of these systems, an alkoxy-substituted derivative, PMPT-OMe, and a non-substituted derivative, PMPT-H, were studied for comparison (Figure 8). As the scan rate increased, the peak potentials of PMPT-OMe shifted minimally as shown in Figure 8 (left), while a significant shift of anodic and cathodic peak potentials was observed in PMPT-H. We observed two oxidation and reduction peaks in the CV of PMPT-OMe similar to that discussed for PMPT-OAc (Figure 4). The oxidation in PMPT-H occurred at a higher potential than PMPT-OMe due to the absence of charge-stabilizing substituents, and peak potentials shifted significantly at fast scan rates. At higher potentials (>1.0 V vs Fc/Fc⁺), PMPT-H was unstable, and hence we were unable to show a peak in the CV. When PMPT-OMe and PMPT-H are compared to PMPT-OH,

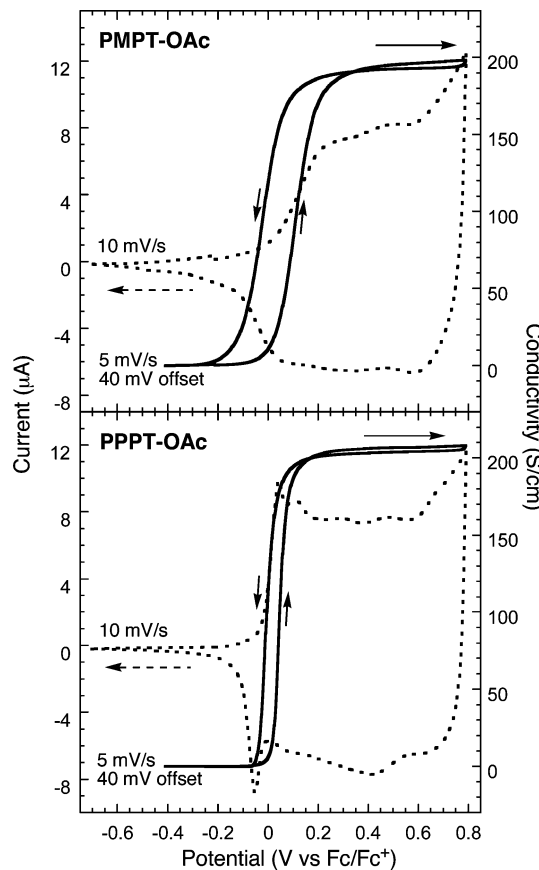


Figure 5. CVs (dotted line) and in-situ conductivity measurements (5 mV/s, offset potential of 40 mV; solid line) of PMPT-OAc (top) and PPPT-OAc (bottom) on 5 μ m interdigitated Pt microelectrodes in CH₂Cl₂ with 0.1 M TBAPF₆ as a supporting electrolyte.

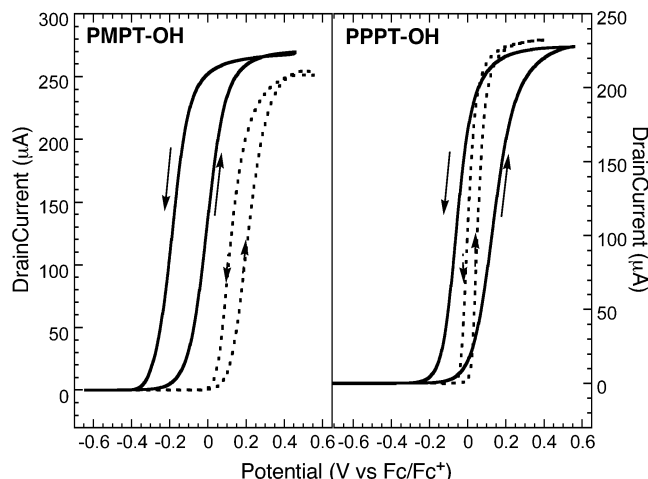


Figure 6. Drain current profiles (5 mV/s, offset potential of 40 mV; solid line) of PMPT-OH and PPPT-OH on 5 μ m interdigitated Pt microelectrodes in CH₂Cl₂ with 0.1 M TBAPF₆ as a supporting electrolyte. The absolute conductivity is proportional to drain current.¹¹ For comparison, drain current profiles of PMPT-OAc (left, dotted line) and PPPT-OAc (right, dotted line) are also plotted.

it is apparent that phenol functionalities enhance the electroactivity of the polymer.

Figure 9 shows the in-situ conductivity measurements of the PMPT-OMe and the PMPT-H. The conductivity–potential profile of PMPT-OMe resembles that of PMPT-OAc and appears to be limited by the interchain charge hopping. However, in PMPT-H, the onset is shifted to

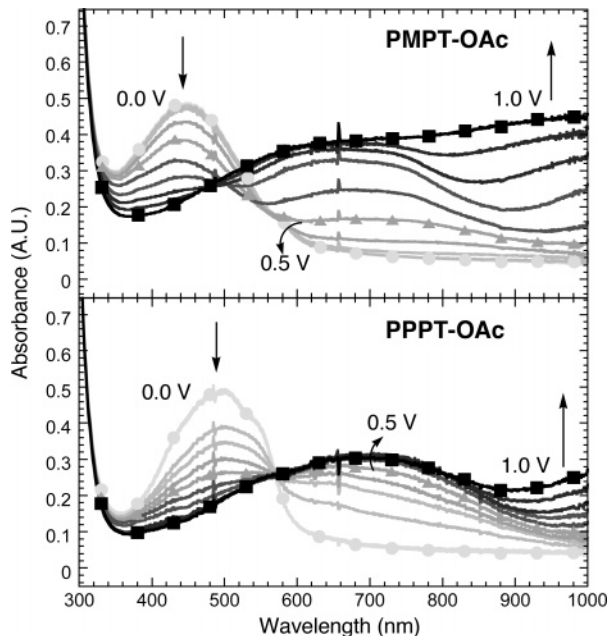


Figure 7. Electronic absorption spectra of PMPT-OAc (top) and PPPT-OAc (bottom) on ITO-coated glass electrodes in CH_2Cl_2 with 0.1 M TBAPF₆ as a supporting electrolyte. The UV-vis spectra are plotted as a function of oxidation potential from 0.0 V (●) to 1.0 V (■) vs Ag/Ag⁺ (0.01 M).

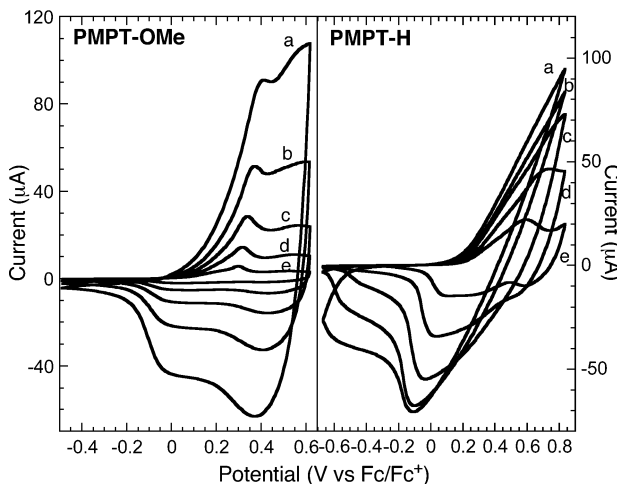


Figure 8. CVs of PMPT-OMe (left) and PMPT-H (right) in CH_3CN and CH_2Cl_2 , respectively, with 0.1 M TBAPF₆ as a supporting electrolyte at different scan rates: (a) 200, (b) 100, (c) 50, (d) 25, and (e) 10 mV/s.

the significantly higher potential, and the conductivity-potential profile passes a peak at ca. 0.55 V and then increases again, finally reaching a plateau at above 0.8 V (vs Fc/Fc⁺). Although there might be a different regime at low potential, or at a low doping level, we suspect that the conductivity of PMPT-H is also governed by the interchain charge hopping at a high doping level. The maximum conductivity of PMPT-OMe and PMPT-OAc was consistently determined to be approximately 2-fold greater than that of PMPT-H.

Spectroelectrochemical studies (Figure 10) reveal approximately the same buildup of energy states as the doping level increases. The UV-vis absorption spectra of PMPT-OMe and PMPT-OAc are similar at the similar oxidation level. Here again, we observed the stabilizing effect of alkoxy functionalities on positively doped states. In PMPT-H, a similar but retarded development of intergap transitions was observed. In addition, the

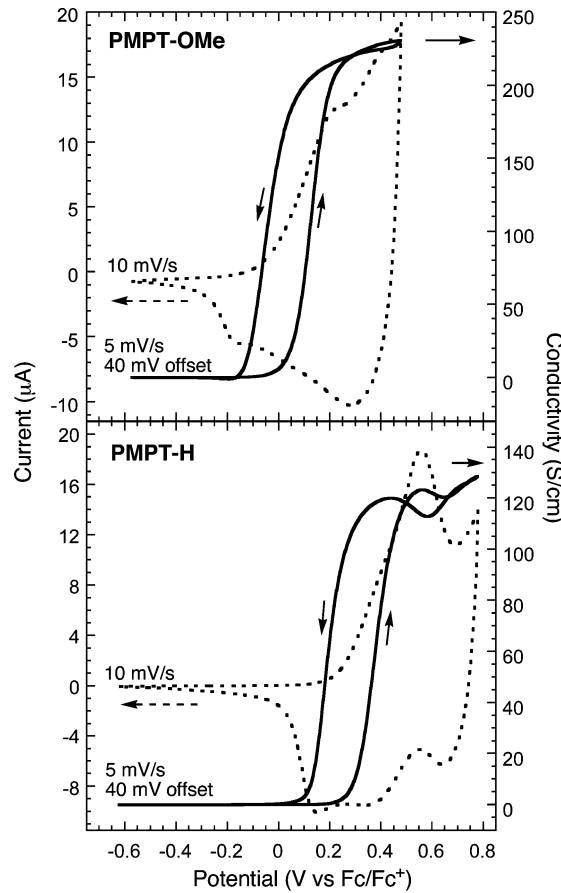


Figure 9. CVs (dotted line) and in-situ conductivity measurements (5 mV/s, offset potential of 40 mV; solid line) of PMPT-OMe (top) and PMPT-H (bottom) on 5 μm interdigitated Pt microelectrodes in CH_2Cl_2 with 0.1 M TBAPF₆ as a supporting electrolyte.

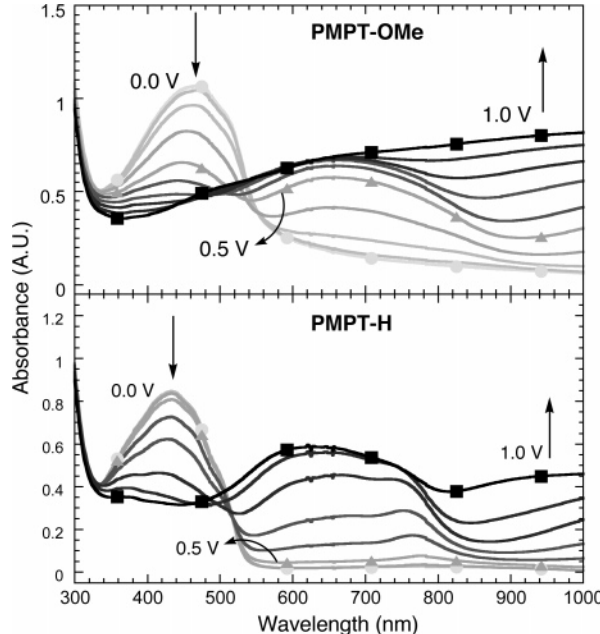


Figure 10. Electronic absorption spectra of PMPT-OMe (top) and PMPT-H (bottom) on ITO-coated glass electrodes in CH_2Cl_2 with 0.1 M TBAPF₆ as a supporting electrolyte, as a function of oxidation potential from 0.0 V (●) to 1.0 V (■) vs Ag/Ag⁺ (0.01 M).

shape of intergap transitions of PMPT-H was different from that of PMPT-OMe or PMPT-OAc (Figure 7, top).

We suspect that without the alkoxy or phenolic substituents delocalized energy states would not be observed in PMPTs at a moderate doping level.

Conclusion

We have found that *meta*-linked polymers can be rendered as electroactive as *para*-linked isomers by strategic positioning of phenolic substituents. The maximum conductivities of both *meta*- and *para*-linked polymers in *in-situ* measurements were similar to each other but appeared to be limited by an interchain charge transport. Spectroelectrochemical studies demonstrated that there were very delocalized energy states in both systems when they were oxidized. Free —OH substituents showed a marked effect on the *meta*-linked polymer over that of the acetoxy or methoxy substituents, resulting in much lower onset potential in a conductivity—potential profile and broad electroactivity of the polymer.

Acknowledgment. We are thankful for funding from DARPA and the Office of Naval Research.

References and Notes

- (1) (a) *Conjugated Polymers*; Bredas, J. L., Silbey, R., Eds.; Kluwer Academic Publishers: Dordrecht, The Netherlands, 1991. (b) *Organic Electronic Materials*; Farchioni, R., Grossi, G., Eds.; Springer: New York, 2001.
- (2) Sato, M.; Tanaka, S.; Kaeriyama, K. *J. Chem. Soc., Chem. Commun.* **1986**, 873.
- (3) Jen, K. Y.; Miller, G. C.; Elsenbaumer, R. L. *J. Chem. Soc., Chem. Commun.* **1986**, 1346.
- (4) Roncali, J. *Chem. Rev.* **1992**, *92*, 711.
- (5) Zotti, G.; Gallazzi, M. C.; Zerbi, G.; Meille, S. V. *Synth. Met.* **1995**, *73*, 217.
- (6) Child, A. D.; Sankaran, B.; Larmat, F.; Reynolds, J. R. *Macromolecules* **1995**, *28*, 6571.
- (7) (a) Sarker, H.; Ong, I.; Sarker, S.; Se arson, P. C.; Poehler, T. O. *Synth. Met.* **2000**, *108*, 33. (b) Pei, J.; Yu, W.-L.; Ni, J.; Lai, Y.-H.; Huang, W.; Heeger, A. J. *Macromolecules* **2001**, *34*, 7241. (c) Bouachrine, M.; Bouzakraoui, S.; Hamidi, M.; Ayachi, S.; Alimi, K.; Lere-Porte, J.-P.; Moreau, J. *Synth. Met.* **2004**, *145*, 237.
- (8) (a) Reddinger, J. L.; Reynolds, J. R. *Macromolecules* **1997**, *30*, 479. (b) Liao, L.; Pang, Y. *Macromolecules* **2001**, *34*, 7300. (c) Hong, S. Y.; Kim, D. Y.; Kim, C. Y.; Hoffmann, R. *Macromolecules* **2001**, *34*, 6474.
- (9) Yu, H.-h.; Xu, B.; Swager, T. M. *J. Am. Chem. Soc.* **2003**, *125*, 1142.
- (10) (a) Jenekhe, S. A. *Nature (London)* **1986**, *322*, 345. (b) Chen, W.-C.; Liu, C.-L.; Yen, C.-T.; Tsai, F.-C.; Tonzola, C. J.; Olson, N.; Jenekhe, S. A. *Macromolecules* **2004**, *37*, 5959.
- (11) (a) Kingsborough, R. P.; Swager, T. M. *Adv. Mater.* **1998**, *10*, 1100. (b) Kingsborough, R. P.; Swager, T. M. *J. Am. Chem. Soc.* **1999**, *121*, 8825.
- (12) Nicolet, B. H.; Sampey, J. R. *J. Am. Chem. Soc.* **1927**, *49*, 1796.
- (13) Zhou, Q.; Swager, T. M. *J. Am. Chem. Soc.* **1995**, *117*, 12593.
- (14) Zhu, S. S.; Swager, T. M. *J. Am. Chem. Soc.* **1997**, *119*, 12568.
- (15) Chemical polymerization with FeCl_3 was attempted but produced insoluble materials that could not be characterized.
- (16) *Electroactive Polymer Electrochemistry*; Lyons, M. E. G., Ed.; Plenum: New York, 1994.
- (17) (a) Miller, L. L.; Mann, K. R. *Acc. Chem. Res.* **1996**, *29*, 417. (b) Cornil, J.; Beljonne, D.; Calbert, J.-P.; Bredas, J. L. *Adv. Mater.* **2001**, *13*, 1053.
- (18) (a) Bredas, J. L.; Street, G. B. *Acc. Chem. Res.* **1985**, *18*, 309. (b) Heeger, A. J.; Kivelson, S.; Schrieffer, J. R.; Su, W.-P. *Rev. Mod. Phys.* **1988**, *60*, 781.

MA0501702